Title
CONCENTRATION PROFILES IN A STEFAN DIFFUSION TUBE

Authors
Heinzelmann, Fred J.
Wasan, Darshanlal T.
Wilke, Charles R.

Publication Date
1964-07-01

UCRL-10421 Rev. 2

University of California

Ernest O. Lawrence Radiation Laboratory

CONCENTRATION PROFILES IN A STEFAN DIFFUSION TUBE

DISCLAIMER

To be published in Industrial and Engineering Chemistry Fundamentals.

UCRL-10421 Rev. 2

UNIVERSITY OF CALIFORNIA

Lawrence Radiation Laboratory
Berkeley, California

AEC Contract No. W-7405-eng-48

CONCENTRATION PROFILES IN A STEFAN DIFFUSION TUBE

Fred J. Heinzelmann, Darshanlal T. Wasan, and Charles R. Wilke

July 1964

CONCENTRATION PROFILES IN A STEFAN DIFFUSION TUBE

Fred J. Heinzelmann, Darshanlal T. Wasan, and Charles R. Wilke

Lawrence Radiation Laboratory and
Department of Chemical Engineering
University of California
Berkeley, California

July 1964

ABSTRACT

The theoretical analysis of the Stefan diffusion tube for measurement of vapor phase diffusion coefficients has conventionally been made with the assumption of plug-flow (flat) concentration profiles in the tube. This assumption has been examined theoretically and experimentally with the conclusion that the radial concentration profile is effectively flat across the diffusion tube. Concentration profiles were estimated by using the Taylor diffusion model. It is also shown theoretically that the shape of the velocity profile does not affect the mass flux provided the concentration profile is flat. Thus diffusion data that have been calculated from Stefan diffusion tube data with the plug flow approximation are substantially correct.

INTRODUCTION

The Stafan diffusion tube has been widely used for the determination of vapor-phase diffusion coefficients. The liquid to be vaporized is placed in the bottom of a vertical tube which is maintained at a constant temperature. A gas is passed over the top of the tube at a rate sufficient enough to keep the partial pressure of the vapor there at the value essentially corresponding to the initial composition of the gas but low enough to prevent turbulence. The mass flux is determined by weighing the tube during the quasi-steady state evaporation period. The vapor-phase diffusion coefficients are readily calculated from the mass flux and concentration gradient over the diffusion path with the assumption of plug flow in the tube. A critical review of the experimental technique has been presented by Lee and Wilke (10).

The equations for isothermal diffusion are well known, having first beed developed by Maxwell (9) and Stefan (13,14). For the ith component, these equations have the form

$$-\frac{P}{RT}\frac{dy_i}{dx} = \sum_{j\neq i}^{n}\frac{N_i y_j - N_j y_i}{D_{ij}} . \qquad (1)$$

This equation, in the case of binary diffusion, which is the case of interest in this study, can be transformed into (16)

$$N_A = \frac{-D_{AB}P}{RT}\frac{dy_A}{dx} + (N_A + N_B)y_A . \qquad (2)$$

This equation defines the vapor-phase diffusion coefficient D_{AB} (2).

With component B stagnant, i.e., $N_B = 0$, the equation becomes

$$N_A = \frac{-D_{AB}P}{RT}\frac{dy_A}{dx} + N_A y_A . \qquad (3)$$

The first term on the right-hand side is the contribution of equimolal diffusion; the second term is interpreted as the contribution to the flux of A due to

the bulk flow set up by the diffusion. Integration of Equation 3, assuming D_{AB} constant, gives (16)

$$N_A = \frac{D_{AB}P\Delta p}{RT\Delta x(p_f)} , \qquad (4)$$

where (p_f) is the diffusion-film-pressure factor. It is defined as

$$p_f = \frac{(P-p_S) - (P-p_0)}{\ell n \ P-p_S/P-p_0} .$$

Equation 4 is used to calculate diffusion coefficients from data obtained in the Stefan tube apparatus.

Inherent in the integration of Equation 3 is the assumption that no radial concentration gradients exist in the Stefan tube. This assumption has not previously been verified. The study presented here involves theoretical analysis of the diffusion system and an experiment designed to determine whether or not the flat-profile assumption is valid.

Analysis of the Diffusion System

Consider the diffusion system as shown in Figure 1. Liquid A evaporates into a stagnant column of gas B. At the liquid-gas interface (x = 0) the gas phase concentration of A, corresponding to equilibrium with the liquid, is denoted by C_s. At the top of the tube (x = L) a stream of gas B flows past slowly. The system is kept at constant temperature and pressure. At steady state there is a net flux of component A away from the evaporating surface and component B is stagnant.

The diffusion system under consideration can be characterized by very slow motion flow. Hence inertial terms can be neglected as suggested by Schlichting (12). Furthermore, if it is assumed that there is a radial symmetry ($V_\theta = 0$) then the basic differential equations of motion can be written as (3)

$$\frac{\partial P}{\partial r} = \nu \left[\frac{\partial}{\partial r} \left(\frac{1}{r} \frac{\partial}{\partial r} (rv) \right) + \frac{\partial^2 v}{\partial x^2} \right], \tag{5}$$

$$\frac{\partial P}{\partial x} = \nu \left[\frac{1}{r} \frac{\partial}{\partial r} \left(r \frac{\partial u}{\partial r} \right) + \frac{\partial^2 u}{\partial x^2} \right]. \tag{6}$$

If Equation 5 is now differentiated with respect to x, and Equation 6 is differentiated with respect to r, and the results are subtracted, one gets

$$\frac{\partial}{\partial x} \left[\frac{\partial}{\partial r} \left(\frac{1}{r} \frac{\partial}{\partial r} (rv) \right) + \frac{\partial^2 v}{\partial x^2} \right] = \frac{\partial}{\partial r} \left[\frac{1}{r} \frac{\partial}{\partial r} \left(r \frac{\partial u}{\partial r} \right) + \frac{\partial^2 u}{\partial x^2} \right]. \tag{7}$$

The pressure term has been eliminated. Now v and u are expressed in terms of the stream function, ψ, according to the following relationship

$$u = -\frac{1}{r} \frac{\partial \psi}{\partial r},$$

$$v = \frac{1}{r} \frac{\partial \psi}{\partial x}.$$

Then Equation 7 is transformed into (12)

$$\nabla^4 \psi = 0, \tag{8}$$

where

$$\nabla^2 \equiv \frac{\partial^2}{\partial r^2} - \frac{1}{r} \frac{\partial}{\partial r} + \frac{\partial^2}{\partial x^2} \tag{9}$$

and

$$\nabla^4 \psi \equiv \nabla^2 (\nabla^2 \psi). \tag{10}$$

Equation 8 is a fourth-order equation in the stream function which automatically satisfies the equation of continuity.

The steady-state diffusion equation for component A with a constant diffusion coefficient and density is (4)

$$v \frac{\partial C_A}{\partial r} + u \frac{\partial C_A}{\partial x} = D \frac{1}{r} \frac{\partial}{\partial r} \left(r \frac{\partial C_A}{\partial r} \right) + D \frac{\partial^2 C_A}{\partial x^2} . \qquad (11)$$

Equation 11 results from the application of conservation of mass and Fick's first law.

Now consider the boundary values of the system.

1. The concentration of A at the liquid-gas interface is constant. Hence

$$C_A = C_S, \text{ a constant at } x = 0 \text{ for all } r.$$

2. The concentration of A at the top of the tube is zero. Hence

$$C_A = 0 \text{ at } x = L \text{ for all } r.$$

3. The concentration profile is symmetrical about the x axis. Hence

$$\frac{\partial C_A}{\partial r} = 0 \text{ at } r = 0 \text{ for all } x.$$

4. There is no transfer from the walls of the tube into the gas. Hence

$$\frac{\partial C_A}{\partial r} = 0 \text{ at } r = r_0 \text{ for all } x.$$

5. There is no slip at the wall. Hence

$$u = 0 \text{ at } r = r_0 \text{ for all } x.$$

6. The velocity profile is symmetrical about the x axis. Hence

$$\frac{\partial u}{\partial r} = 0 \text{ at } r = 0 \text{ for all } x.$$

7. At the evaporating surface the diffusion velocity is related to the concentration gradient of the diffusing species by

$$u = - \frac{D}{C_B} \left(\frac{\partial C_A}{\partial x} \right) \text{ at } x = 0 \text{ for all } r.$$

The above equations assume that the mass average velocity is equal to the mole average velocity. This is ture only when the molecular weight of A equals that of B. However, for low mass-transfer rates the assumption introduces little error and is satisfactory.

The coupling between momentum equation (Equation 8) and the diffusion equation (Equation 11) is provided by the boundary condition 7. The simultaneous solution of Equations 8 and 11 satisfying all the boundary conditions provides the exact solutions for the velocity $u(x,r)$ and concentration $C(x,r)$ distributions in the Stefan diffusion tube. However, the solution is extremely difficult and probably can be only obtained numerically on a computer.

In the absence of a more rigorous solution we can estimate the concentration profiles in the Stefan diffusion tube by using the Taylor diffusion model (15). This is, of course, only a limiting case, but one which should give the correct order of magnitude for any radial non-uniformity in concentration. In this model it is assumed that the usual parabolic velocity profile for laminar flow develops at once and remains undisturbed over the length of the tube. Also, it is necessarily assumed that there is no slip at the wall. These are believed to be satisfactory limiting assumptions since they represent the maximum departure from plug flow. Taylor considered the dispersion of a solute into a fluid in laminar flow through a tube. The distribution of concentration of the solute depends on the balance between the molecular diffusion and the convection due to variation in velocity over the cross-section. The transport equation according to Taylor can be taken as

$$\frac{\partial^2 C}{\partial r^2} + \frac{1}{r}\frac{\partial C}{\partial r} = \frac{1}{D}\frac{\partial C}{\partial t} + \frac{U}{D}\left[1 - 2\,(r/r_0)^2\right]\frac{\partial C}{\partial x} \qquad (12)$$

where U is the average velocity. In obtaining Equation 12 axial diffusion is assumed to be negligible. Aris (1) extended the analysis of Taylor to include the effect of axial diffusion. His results show that for the purpose of present calculations this assumption introduces little error.

Taylor presented an approximate solution of Equation 12 under the condition that the time necessary for appreciable effects to appear, owing to convective transport, is long compared with the time of decay during which radial variation of concentration are reduced to a fraction of their initial value through the action of molecular diffusion. This condition can be expressed as

$$\frac{L}{D} >> \frac{2(r_0)^2}{(3.8)^2 D} \quad . \tag{13}$$

The term $r_0^2/(3.8)^2 D$ represents the time necessary for a non-uniform concentration to degenerate into an essentially uniform concentration.

According to Taylor the small radial variation in the concentration, C, can be calculated from the equation

$$\frac{\partial^2 C}{\partial r^2} + \frac{1}{r}\frac{\partial C}{\partial r} = \frac{2(r_0)^2 U}{D}\left[\frac{1}{2} - \left(\frac{r}{r_0}\right)^2\right]\left(\frac{\partial C}{\partial x_1}\right)_{r=0} \tag{14}$$

where

$$x_1 = x - Ut \tag{15}$$

and in this calculation $(\partial C/\partial x_1)_{r=0}$ may be taken as independent of r.

A solution of Equation 15 which satisfies the boundary condition (4) is

$$C(x,r) = C_{x_1} + \frac{2(r_0)^2 U}{8D}\left(\frac{\partial C}{\partial x_1}\right)_{r=0}\left[\left(\frac{r}{r_0}\right)^2 - \frac{1}{2}\left(\frac{r}{r_0}\right)^4\right] . \tag{16}$$

The longitudinal dispersion of solute can be described by the differential equation as given by (15)

$$k \frac{\partial^2 C}{\partial x_1^2} = \frac{\partial C}{\partial t} \qquad (17)$$

where k is the diffusion coefficient.

The solution of Equation (17) for the present analysis is

$$\frac{C}{C_S} = \frac{1}{2} - \frac{1}{2} \text{ erf } \left(\frac{1}{2} x_1 k^{-1/2} t^{-1/2}\right) \qquad (18)$$

where erf(Z) is an Error function. Hence the concentration profiles can be estimated from equations 16 and 18 as

$$\frac{C}{C_S} = \frac{1}{2} - \frac{1}{2} \text{ erf } \left(\frac{1}{2} x_1 / \sqrt{kt}\right) - \frac{1}{2\sqrt{kt\pi}} \frac{(r/r_0)^2 U}{4D} e^{-\left(\frac{x_1}{2}\sqrt{\frac{1}{kt}}\right)^2}$$

$$\left[(r/r_0)^2 - \frac{1}{2}(r/r_0)^4\right]. \qquad (19)$$

The second term on the right-hand side of Equation 19 represents the concentration variation in the radial direction. In order to calculate the radial concentration distribution in the Stefan diffusion tube a value of C/C_S is chosen corresponding to a given value of x and Equation (15) is substituted for x_1 in Equation 19 and time t is determined. Then the radial concentration profile is estimated. These values are compared with the flat concentration profiles given by the equation

$$\frac{C^*}{C_S} = \frac{1 - \exp[(U/D)(L-x)]}{1 - \exp(UL/D)} \qquad (20)$$

where : C^* is hypothetical uniform concentration across r at given x; Equation 20 is the solution (11) of diffusion Equation (11) with the conditions that there is no radial velocity V and the velocity profile is flat across the radius of the tube.

APPARATUS

The apparatus used in this study is shown schematically in Figure 2. The diffusion system is substantially the same as that used in recent measurements of diffusion coefficients and is described in detail by Getzinger (5). However, a probe and electronic recording equipment have been added to measure the concentration profiles.

Diffusion System. The diffusion unit is shown schematically in Figure 3. The air enters the diffusion unit through straightening vanes to eliminate turbulence before passing over the diffusion tube. The diffusion unit was constructed of brass. Leads are provided to connect the probe and the electrical measuring devices.

The diffusion tube itself was designed to give a diffusion area with 1-in. i.d. The diffusion tube was built with a step design. The bottom was 1-in. i.d. and the top a 1.50-in. i.d. to accommodate the probe. With the probe in place the top part also had a 1-in. i.d. providing a smooth diffusion tube.

The probe was not extended to the bottom of the diffusion tube, so that liquid was prevented from rising up between the probe and the diffusion tube wall by capillary action (preliminary experiments had shown this to be a problem).

With the probe in place, the actual diffusion area was an uniform 1-in. i.d circular cross section. An aluminum sleeve was used over the bottom of the diffusion tube to get a uniform outside diameter of 1.535 in. This gave a tight fit within the diffusion-tube holder, providing good thermal contact.

The diffusion tube itself was constructed with a wall thickness of only 0.018 in. This made the assembly light enough to be weighed on the analytical balance in the laboratory to determine the weight loss by evaporation during a run.

Measurements were made of the time required to reach thermal equilibrium in the system. After only 15 minutes the gas temperature as measured by

a conventional mercury thermometer was found to be within 0.1°C of the bath temperatures.

Air enters the system at room temperature from compressed air cylinders through a three-stage pressure regulator. It is then dried with an isopropyl alcohol-dry ice trap and is then further dried with a 6-in. column of Drierite. After passage through a flowrator, it is heated by an electric heating element to about 32°C. The air is then passed through 40 feet of copper tubing immersed in a constant-temperature bath, where it is heated to 35.0 ± 0.1°C, the temperature used in the experiments. The diffusion unit is also immersed in the constant-temperature bath to insure isothermal operation. After passing through the diffusion unit the air is exhausted through a blower to the outside.

The constant-temperature bath is a 12-in.-diameter by 16-in.-deep Pyrex jar housed in a large wooden box insulated with Styrofoam. The bath temperature is maintained at 35.0 ± 0.1°C by an electric heating element regulated by a mercury thermoregulator connected to a specially built controller. The temperature was chosen to give a reasonably high vapor pressure for the benzene, the liquid used in the experiment. The bath is agitated by a Variac-controlled variable-speed General Electric motor driving a specially built propeller.

Probe. To measure the concentration profiles in the diffusion tube semicircular probes were used. The principle of the probe operation is the same as that of a thermal-conductivity cell. The detailed study of the optimum probe design is given elsewhere (7). Because of the radial symmetry of the diffusion system these probes could be used to measure the radial concentration gradients. Three probes were constructed, each of different diameter. The dimensions are given in Table I. A picture of probe 1 is shown in Figure 4.

The probes were constructed with an aluminum ring as the primary support. The probe itself was constructed of 0.000475-in. diameter cleaned tungsten wire obtained from the Wah Chang Corp. of New York. Thin glass

capillaries were used to support the probe wire and maintain its semi-circular shape.

Table I. Probe dimensions

Probe	Nominal diameter (in.)	Distance from tube wall (in.)	Maximum dev. from diameter (in.)	Nominal resistance (ohms)
1	3/4	4/32	± 1/16	24
2	9/16	7/32	± 1/32	18
3	7/16	9/32	< ± 1/32	15

The probe was placed in the diffusion tube along with three 1-in.-high 1-in. aluminum rings. The vertical position of the probe was changed by moving its position among these rings. All these aluminum rings had a machined inner surface of 1-in. i.d. in order to provide a smooth diffusion tube.

EXPERIMENTAL PROCEDURE

Benzene was chosen to be the diffusing substance and air as the gaseous diffusion medium. These were selected because considerable diffusion data have been obtained for these components in the Stefan-tube apparatus. Also these components have considerably different thermal conductivities, thus giving a reasonably good probe sensitivity. The temperature of the system was chosen at 35°C to give a reasonable vapor pressure and thus a significant mass flux.

The air flow rate over the diffusion tube was chosen to give minimum end effects due to turbulence at the top of the diffusion tube, but high enough to insure that stagnation did not take place. Preliminary experiments indicated that the air flow rate for this system should be about 120 cc/min, giving a velocity of 4.65 cm/sec through the straightening vanes in the diffusion system. This is somewhat lower than the gas rate used in Stefan-tube studies by

Getzinger (5). A lower gas rate was required because of increased turbulence in the diffusion system due to the presence of the probe leads. The gas rate fixed the operating pressure at 1.6 to 2.0 in. of water above atmospheric pressure.

After the air flow rate was determined some runs were made on the system without the probe in place, in order to determine the characteristics of the system. After these runs were finished runs were made with the probe in place. Data were taken with each probe in three vertical positions. Probe resistances were measured by using a Wheatstone bridge and Brush amplifier and recorder to measure the bridge balance.

When measurements were made of the probes the time used was as short as possible, in order to aboid setting up convection currents in the system. Several readings were made of each run, since making good electrical contacts proved to be a problem. The probes were calibrated in calibration cells with known gas compositions.

Benzene loss in the Stefan diffusion tube was determined by weighing the tube before and after each run. Weights were determined to the nearest 0.001 g. While out of the system the tube was kept stoppered at all times to prevent evaporation of benzene. Liquid depth in the tube was determined from the weight of benzene. Most runs lasted more than 3 hours. A few runs were only 30 to 40 minutes. Although it has been estimated that equilibrium is reached in 15 minutes (10), these shorter runs gave badly scattered points and were discarded.

RESULTS AND DISCUSSION

Theoretical Results. Using the values D = 0.11 cm^2/sec, L = 13 cm, and U = 0.00186 cm/sec the time required for the radial variation of concentration represented by Equation 13 to degenerate into a uniform concentration is found to be of the order of one second whereas the time necessary for convection to make an appreciable change in C is of the order of one hour.

Radial concentration profiles were estimated from Equations 15 and 19. The values of the ratio $\frac{C^*-C(r)}{C^*}$ at several values of the radial and axial distances are shown in Table II.

Table II. Radial variation in concentration, $C^*-C(r)/C^*$ at various positions in the tube.

$r/r_0 \rightarrow$	0	0.24	0.71	0.87
	$\frac{C^*-C(r)}{C^*}$	$\frac{C^*-C(r)}{C^*}$	$\frac{C^*-C(r)}{C^*}$	$\frac{C^*-C(r)}{C^*}$
7.54	0	-1.6×10^{-3}	-1.1×10^{-2}	-1.4×10^{-2}
13	0	0	0	0

It is noted that the deviation of the radial concentration from a uniform value did not exceed 1.4% in positions chosen for calculation. Although a somewhat larger deviation could exist at other positions, and particularly near the wall, we believe that the calculations indicate that the concentration is essentially uniform across the radius of the tube for all practical purposes. Thus the flat concentration profile that has been assumed in past interpretations of Stefan-tube data appears quite satisfactory for diffusion coefficient measurements.

Now consider a diffusion tube with no radial concentration gradient but with some radial velocity distribution. Component A is diffusing through stagnant component B. In a thin cylindrical section, which has a constant velocity u(r), the mass flux is given by

$$N_A = -D \frac{\partial C_A}{\partial x} + u(r)C_A. \tag{21}$$

This is equivalent to Equation 3. The total mass transfer is found by integrating over all values of r, or

$$J_T = \int_0^{r_0} N_A 2\pi r dr = 2\pi \int_0^{r_0} -D \frac{dC_A}{dx} r dr + 2\pi \int_0^{r_0} C_A u(r) r dr. \tag{22}$$

Since C_A is not a function of r, one gets

$$J_T = -D \left(\frac{\partial C_A}{\partial x} \right) \pi r_0^2 + u_0 \pi r_0^2 C_A \tag{23}$$

$$N_A = \frac{J_T}{\pi r_0^2} = -D \frac{\partial C_A}{\partial x} + u_0 C_A. \tag{24}$$

Equation 24 is the same equation one gets by assuming plug concentration and velocity profiles. This can be integrated to give Equation 4.

Experimental Verification. The concentration profile measured by the probes is shown on Figure 5 and summarized on Table III. One can see that within the experimental error there is no radial concentration gradient.

The concentration gradient in x is of interest, since the values for large x (near the top of the tube) fall on the theoretical line but the points nearest the bottom of the tube indicate a considerably higher concentration than expected.

Table III. Results obtained in determination of concentration profile.

Probe 1					
Run	19M	20M	21M	22M	38M
% Benzene	5.6	9.1	7.8	16.5	6.5
Probe depth (cm)	2.84	5.36	5.36	7.88	2.84
C/C_s	0.28	0.46	0.39	0.83	0.33
Fraction of diffusion distance	0.78	0.58	0.59	0.39	0.78

Probe 2			
Run	15M	16M	17M
% Benzene	8.3	5.8	17.3
Probe depth (cm)	5.36	2.84	7.88
C/C_s	0.42	0.29	0.87
Fraction of diffusion distance	0.58	0.78	0.37

Probe 3			
Run	25M	26M	27M
% Benzene	5.1	6.3	9.0
Probe depth (cm)	2.84	2.84	5.36
C/C_s	0.26	0.32	0.45
Fraction of diffusion distance	0.77	0.77	0.59

Probe 4			
Run	29M	31M	33M
% Benzene	16.1	16.9	6.6
Probe depth (cm)	7.88	7.88	2.84
C/C_s	0.81	0.85	0.33
Fraction of diffusion distance	0.38	0.38	0.78

These points were rechecked and consistently gave the same results. Runs were made in which the probe measurements were made in air saturated with benzene by shutting off the system air flow. When the air flow was started again and the system had reached equilibrium these high values were again obtained.

Diffusion coefficients were also calculated from the data. The true diffusion coefficient, corrected for end effects, was found to be 0.097 cm^2/sec. This value is somewhat lower than the value of 0.103 cm^2/sec obtained from the measurements by Lee and Wilke (10) corrected to our conditions. Since some inaccuracies might be expected in our experiment because of interference by the probes, the former measurements are considered preferable. The detailed experimental data are available elsewhere (7).

The correction for end effects, Δx, was found to be 2.04 cm. This is quite large, and offers a possible explanation for the unexpectedly high concentration values near the bottom of the diffusion tube. If this whole end correction is applied to the bottom of the tube, then the predicted concentration profile and the data points are as shown on Figure 6. The data at the bottom of the table are now much closer to the expected line, but the data at larger values of x now show some deviation from the predicted values. However, on the average, this does give a better fit to the data.

A possible cause of the large end effect at the bottom of the tube may be found in the diffusion thermo effect, according to which a temperature gradient is set up by a concentration gradient. This effect has been observed experimentally, and temperature differences of several degrees centigrade may be set up (8).

In a binary mixture with a diffusion flow of component 1 there exists a heat flow

$$J_H = -\alpha' \, knT \, \text{grad} \, N', \qquad (25)$$

where n is the total concentration of molecules 1 and 2, and N' is the mole fraction of molecule 1. The diffusion thermo-effect coefficient, α', for ideal mixtures is related to the thermal diffusion constant, α, by (6)

$$\alpha' = -D\alpha.$$

Since benzene is the larger and heavier molecule, one would expect α to be positive (i.e., benzene would diffuse toward the cooler end in thermal diffusion). Therefore α' would be negative. Thus, in Equation 25, with grad N' also negative, the heat flux and the higher temperature would be near the bottom of the tube. Thus, one would have a cooler heavier gas on top of a warmer gas layer, starting convection currents. This could cause some flow disturbance at the bottom of the tube and might explain the data points. Further work is required to confirm this.

Another theoretical cause for convective flow in the tube might be gravitational forces due to density gradients associated with any non-uniformity in the concentration over radial position. However, in view of the very small variation in radial concentrations which can develop, as shown in Table II, we believe that such free convection effects would be negligible.

CONCLUSIONS

Theoretical and experimental studies confirm that there is no significant radial concentration gradient in the Stefan diffusion tube. From these results it is concluded that equations developed from the plug flow model for the Stefan-tube may be used to calculate diffusion coefficients. However, it appears possible that end effects can be appreciable, and that therefore a sufficiently long tube should be employed to minimize this influence.

ACKNOWLEDGMENT

This study was conducted under the auspices of the U. S. Atomic Energy Commission.

NOMENCLATURE

C	molar concentration
C^*	concentration with assumption of plug flow
D	diffusion coefficient
J_H	heat flux
J_T	total mass flow
L	length of the diffusion tube
N	mass flux
p	partial pressure
P	total pressure
r_0	radius of tube
r	radial distance
R	gas constant
T	temperature
τ	shear stress
u	velocity in the x direction
U	average velocity
v	velocity in the r direction
x	axial distance
p_s	vapor pressure corresponding to surface temperature
p_0	vapor pressure of the inlet gas
ν	kinematic viscosity
μ	absolute viscosity

LITERATURE CITED

(1) R. Aris, Proc. Roy. Soc. A235, 67 (1956).

(2) R. B. Bird, W E. Stewart, and E. N. Lightfoot,"Transport Phenomena (John Wiley and Sons, Inc., New York, 1960)p.502.

(3) Ibid., p.85.

(4) Ibid., p. 559.

(5) R. W. Getzinger, Steady-State Diffusion in Ternary Gas Mixtures, (M.S. Thesis), University of California, 1962.

(6) R. Hasse, Z. Physik 127, 1 (1950).

(7) F. J. Heinzelmann, D. T. Wasan, and C. R. Wilke, UCRL-10421 (1962).

(8) W. Jost, "Diffusion in Solids, Liquids, and Gases", 3rd Printing (Academic Press, Inc., New York, 1960)p.520.

(9) J. C. Maxwell, "Scientific Papers" (Dover, New York, 1952) Vol. 2.

(10) C. Y. Lee and C. R. Wilke, Ind. Eng. Chem. 46, 2381 (1954).

(11) H. S. Mickley, T. K. Sherwood, and C. E. Reed "Applied Mathematics in Chemical Engineering", 2nd Ed. (McGraw-Hill Book Company, Inc., New York, 1957)p. 153.

(12) H. Schlichting, "Boundary Layer Theory" (McGraw-Hill Book Company, Inc., New York, 1955) p. 83.

(13) J. Stefan, Sitzber. Akad. Wiss, Wien, Math.-naturw. Kl. 63, Abt II (1871)

(14) Ibid., 65, Abt II, 323 (1872).

(15) G. I. Taylor, Proc. Roy. Soc. A219, 186 (1953).

(16) C. R. Wilke, Chem. Eng. Progr. 46, 95 (1950).

FIGURE CAPTIONS

Fig. 1. Schematic diagram of the theoretical model.

Fig. 2. Schematic diagram of the apparatus.

Fig. 3. Diffusion unit.

Fig. 4. Probe 1.

Fig. 5. Experimental concentration profile.

Fig. 6. Experimental concentration profile corrected for end effects.

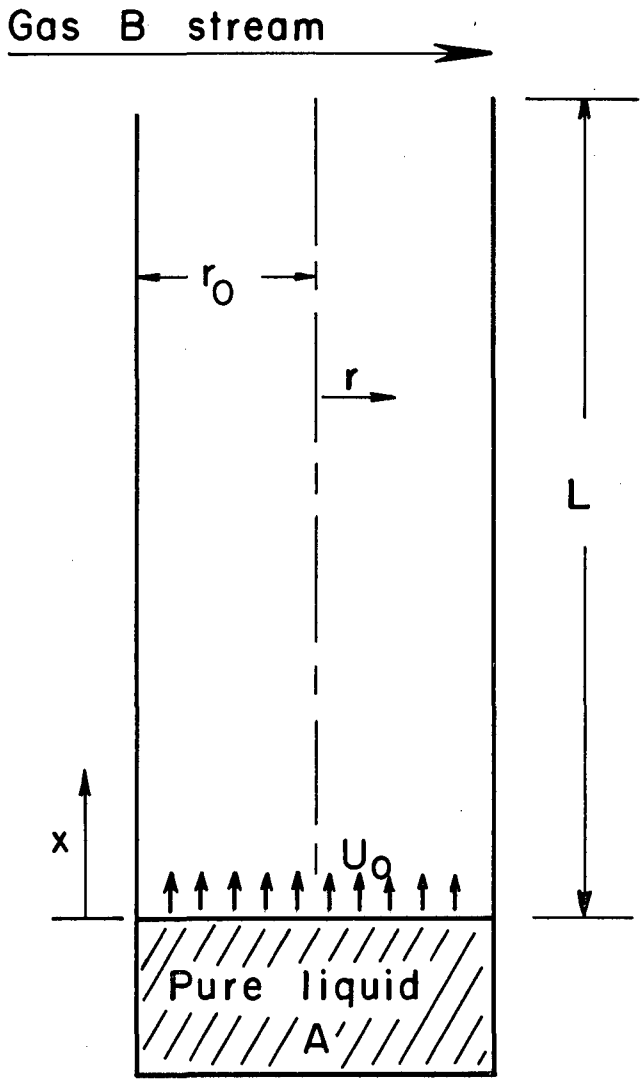

Fig. 1

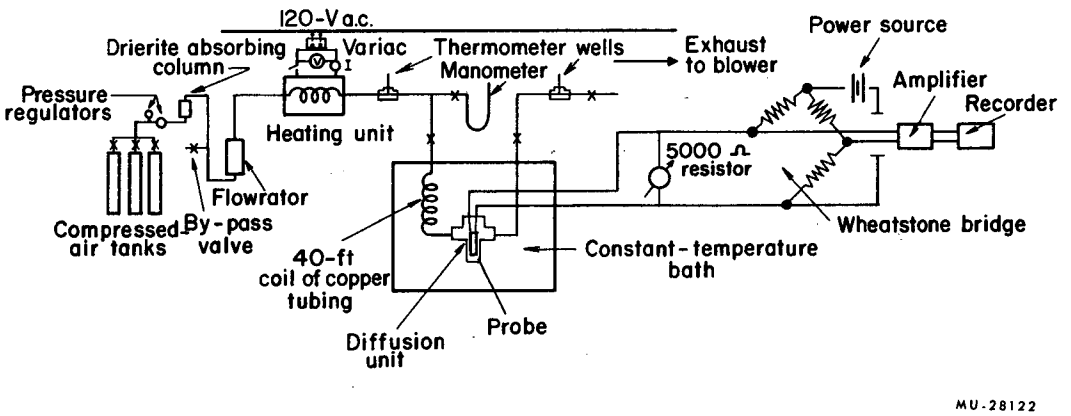
120-V a.c.
Drierite absorbing column
Variac
Thermometer wells
Manometer
Exhaust to blower
Power source
Amplifier
Recorder
Pressure regulators
Heating unit
5000 Ω resistor
Flowrator
By-pass valve
Compressed air tanks
Wheatstone bridge
40-ft coil of copper tubing
Constant-temperature bath
Diffusion unit
Probe
MU-28122

Fig. 2

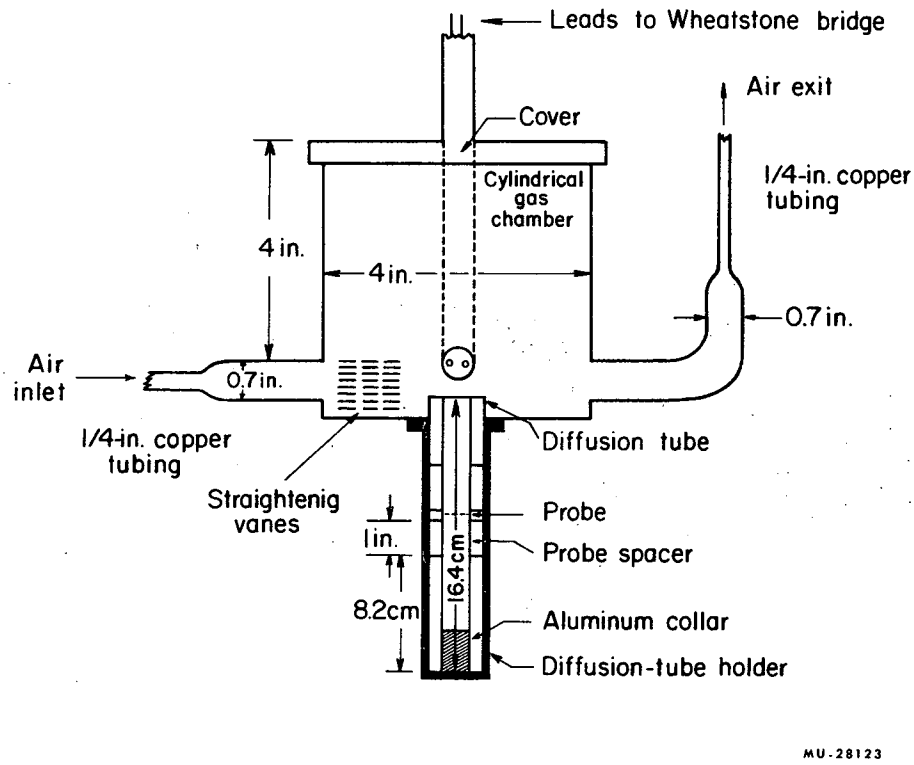
Leads to Wheatstone bridge
Air exit
Cover
Cylindrical gas chamber
1/4-in. copper tubing
4 in.
4 in.
0.7 in.
Air inlet
0.7 in.
1/4-in. copper tubing
Straightenig vanes
Diffusion tube
Probe
Probe spacer
1 in.
16.4 cm
8.2 cm
Aluminum collar
Diffusion-tube holder
MU-28123

Fig. 3

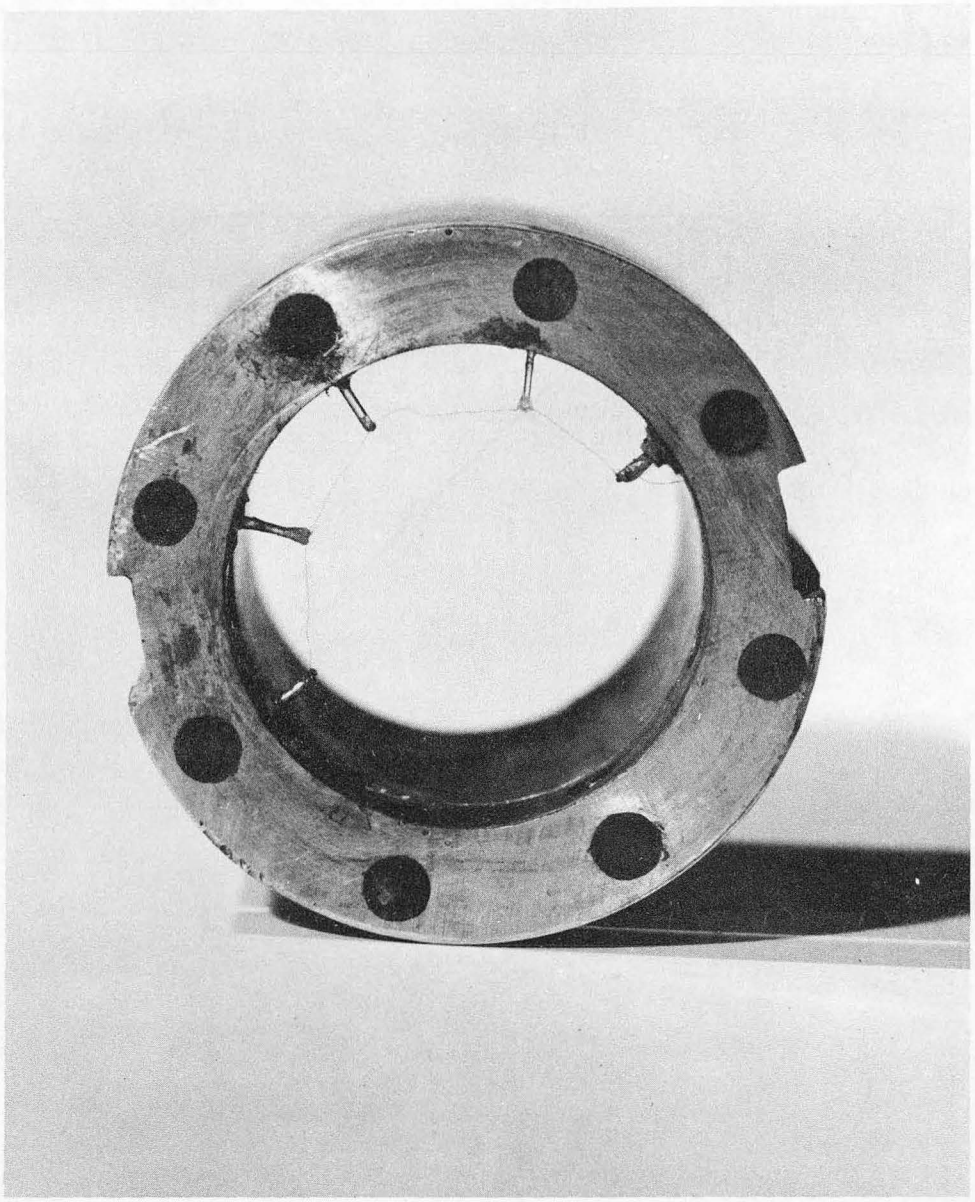

ZN-3358

Fig. 4

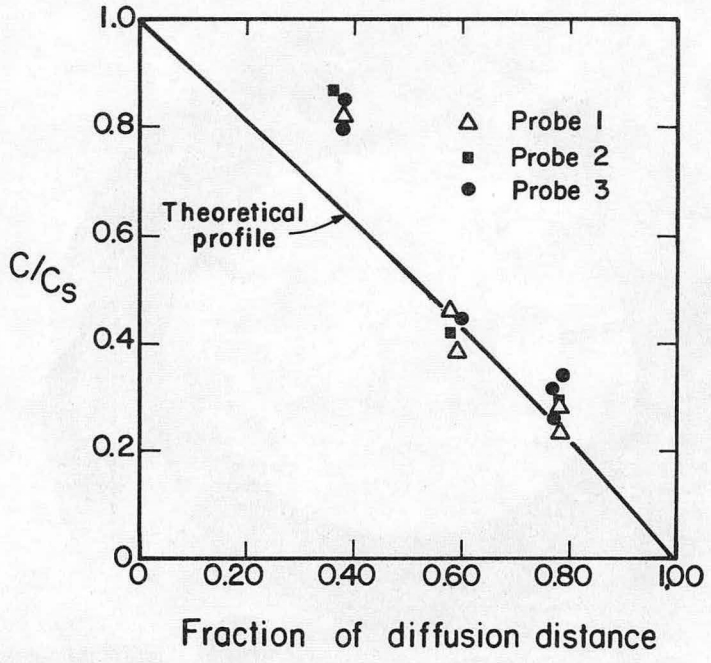
1.0
0.8
0.6
0.4
0.2
0
C/Cs
Theoretical profile
Probe 1
Probe 2
Probe 3
0
0.20
0.40
0.60
0.80
1.00
Fraction of diffusion distance
MU-28134

Fig. 5

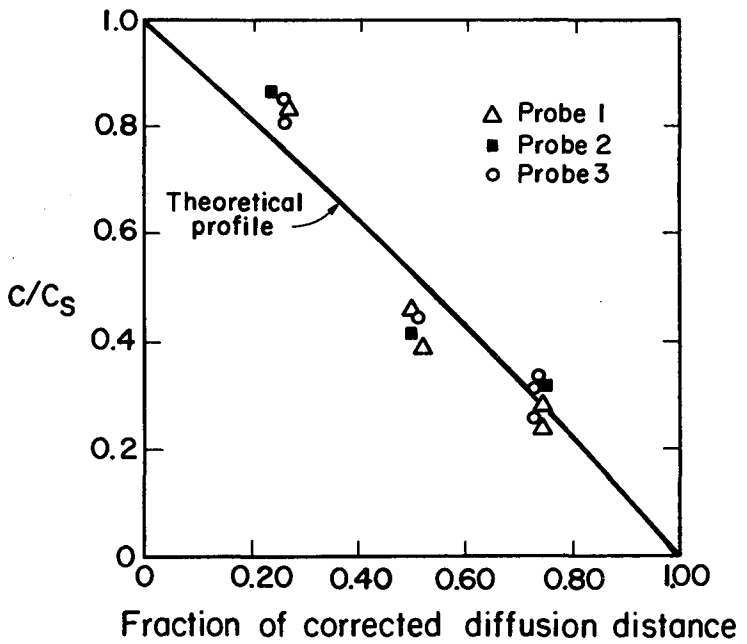
1.0
0.8
0.6
0.4
0.2
0
C/Cs
Theoretical profile
Probe 1
Probe 2
Probe 3
0
0.20
0.40
0.60
0.80
1.00
Fraction of corrected diffusion distance
MU-28135

Fig. 6